ResearchGate

See discussions, stats, and author profiles for this publication at: https://www.researchgate.net/publication/225288898

Decisive Role of Hydrophobic Side Groups of Polypeptides in Thermosensitive Gelation

ARTICLE *in* BIOMACROMOLECULES · JUNE 2012

Impact Factor: 5.75 · DOI: 10.1021/bm3004308 · Source: PubMed

CITATIONS
35

READS
40

7 AUTHORS, INCLUDING:

Yilong Cheng
University of Washington Seattle
18 PUBLICATIONS **364** CITATIONS
SEE PROFILE

Chunsheng Xiao
Chinese Academy of Sciences
73 PUBLICATIONS **1,351** CITATIONS
SEE PROFILE

Jianxun Ding
Chinese Academy of Sciences
102 PUBLICATIONS **1,086** CITATIONS
SEE PROFILE

Yubin Huang
Chinese Academy of Sciences
143 PUBLICATIONS **1,497** CITATIONS
SEE PROFILE

Available from: Yubin Huang
Retrieved on: 26 January 2016

Article

pubs.acs.org/Biomac

Decisive Role of Hydrophobic Side Groups of Polypeptides in Thermosensitive Gelation

Yilong Cheng,[†,‡] Chaoliang He,[†] Chunsheng Xiao,[†] Jianxun Ding,[†,‡] Xiuli Zhuang,[†] Yubin Huang,[†] and Xuesi Chen*[,†]

[†]Key Laboratory of Polymer Ecomaterials, Changchun Institute of Applied Chemistry, Chinese Academy of Sciences, Changchun 130022, People's Republic of China

[‡]Graduate University of Chinese Academy of Sciences, Beijing 100039, People's Republic of China

Supporting Information

ABSTRACT: Thermosensitive hydrogels based on PEG and poly(L-glutamate)s bearing different hydrophobic side groups were separately synthesized by the ring-opening polymerization (ROP) of L-glutamate *N*-carboxyanhydrides containing different alkyl protected groups, that is, methyl, ethyl, *n*-propyl, and *n*-butyl, using $mPEG_{45}$-NH_2 as macroinitiator. The resulting copolymers underwent sol−gel transitions in response to temperature change. Interestingly, the polypeptides containing methyl and ethyl showed significantly lower critical gelation temperatures (CGTs) than those bearing *n*-propyl and butyl side groups. Based on the analysis of ^{13}C NMR spectra, DLS, circular dichroism spectra, and ATR-FTIR spectra, the sol−gel transition mechanism was attributed to the dehydration of poly(ethylene glycol) and the increase of *β*-sheet conformation content in the polypeptides. The in vivo gelation test indicated that the copolymer solution (6.0 wt %) immediately changed to a gel after subcutaneous injection into rats. The mass loss of the hydrogel in vitro was accelerated in the presence of proteinase K, and the MTT assay revealed that the block copolymers exhibited no detectable cytotoxicity. The present work revealed that subtle variation in the length of a hydrophobic side group displayed the decisive effect on the gelation behavior of the polypeptides. In addition, the thermosensitive hydrogels could be promising materials for biomedical applications due to their good biocompatibility, biodegradability, and the fast in situ gelation behavior.

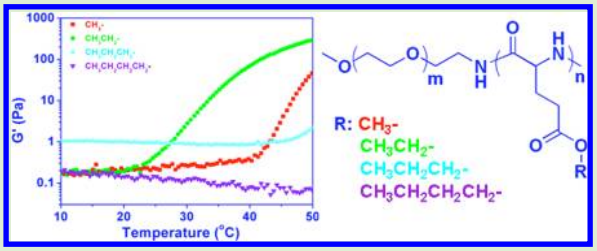

INTRODUCTION

In the past decades, thermosensitive hydrogels have been attractive materials for biomedical applications including drug delivery, tissue engineering scaffolds and prevention of post-surgical adhesion.[1−5] Especially thermoinduced in situ forming biodegradable hydrogels have received considerable attention in recent years, which are mainly based on block copolymers composed of a hydrophilic poly(ethylene glycol) (PEG) block and a hydrophobic biodegradable block, such as poly (lactic acid) (PLA),[6,7] poly(lactic acid-*co*-glycolic acid) (PLGA),[8,9] poly(*ε*-caprolactone) (PCL),[10] poly(*ε*-caprolactone-*co*-lactide) (PCLA),[11] poly((*R*)-3-hydroxybutyrate) (PHB),[12] poly-(amidoamine) (PAA),[13] and so on. At a lower temperature, these systems enable bioactive agents or cells to be simply mixed with polymer solutions, and drug or cell encapsulated hydrogels can be formed at the target site with minimal invasion to act as a sustained drug delivery depot or a three-dimensional matrix for cells proliferation or growth to a tissue.[14−17]

Polypeptide-based biomaterials have drawn increasing interest due to their well-defined secondary structures, good biocompatibilities, and biodegradabilities.[1,18−20] Recently, thermosensitive hydrogels based on block copolymers of hydrophobic polypeptides and hydrophilic PEG or poloxamer have been developed by Jeong and co-workers.[21,22] In comparison with polyester-based thermogelling hydrogels, polypeptide-based systems showed relatively low critical gelation concentrations (CGC) and caused no acidic micro-environment after degradation, which may lead to an adverse effect on the activity of encapsulated protein drugs or cells. In addition, the gelation behavior of polypeptide-based copolymers could be adjusted by varying the secondary structure (*α*-helix, *β*-sheet, and random coil) or by the copolymerization of different hydrophobic and hydrophilic amino acid monomers.

It has been shown that end-capping of polypeptides by hydrophobic groups displayed marked influence on the solution behavior and secondary structure of the polypeptides.[23] However, there are few reports aimed at disclosing the influence of subtle change in the hydrophobicity of the side group of polypeptides on the sol−gel transitions of their solutions. In this work, we have presented four kinds of poly(ethylene glycol)-*block*-poly(L-glutamate)s with different hydrophobic side groups, that is, methyl, ethyl, *n*-propyl, and *n*-butyl, on the poly(L-glutamate) blocks and studied the role of side groups in promoting gel formation. In addition, the in vivo

Received: March 19, 2012
Revised: June 3, 2012
Published: June 8, 2012

 © 2012 American Chemical Society

gel formation, in vitro gel duration, and cytotoxicity of these copolymers were also evaluated.

EXPERIMENTAL SECTION

Materials. Poly(ethylene glycol) monomethyl ether (mPEG, M_n = 2000) was purchased from Aldrich and used without further purification. The amino group terminated poly(ethylene glycol) monomethyl ether (mPEG-NH_2) was synthesized according to our previous literature.[24] THF and toluene were refluxed with sodium and distilled under nitrogen prior to use. *N*,*N*-Dimethylformamide (DMF) was stored over calcium hydride (CaH_2) and purified by vacuum distillation. All the other reagents and solvents were purchased from Sinopharm Chemical Reagent Co. Ltd., China, and used as obtained.

Characterization. ^{1}H NMR spectra of γ-alkyl-L-glutamates in deuterium oxide (D_2O), γ-alkyl-L-glutamates *N*-carboxyanhydrides in deuterated chloroform ($CDCl_3$) and poly(ethylene glycol)-*b*-poly(γ-alkyl-L-glutamate)s in deuterated trifluoroacetic acid (CF_3COOD) were recorded on a Bruker AV 400 NMR spectrometer. ^{13}C NMR spectral changes of PEG_{45}-$PELG_{12}$ (6.0 wt % in D_2O) were investigated as a function of temperature in the range of 20−60 °C, and the solution temperature was equilibrated for 20 min before measurement. ATR-FTIR spectra were recorded for 6.0 wt % polymer solutions in D_2O. The internal reflection element was a zinc selenide ATR plate. To analyze their secondary structure, deconvolution of the FTIR spectra was performed in the amide I band region of 1600−1700 cm^{-1}. The deconvoluted spectra were fitted with Gaussian−Lorentzian sum function (20% Gaussian and 80% Lorentzian) using XPSPEAK software 4.1. Number-average molecular weights (M_n) and polydispersity indexes (PDI) were determined by gel permeation chromatography (GPC) using a series of linear Tskgel Super columns (AW3000 and AW5000) and Waters 515 HPLC pump with OPTILAB DSP Interferometric Refractometer (Wyatt Technology) as the detector. The eluent was DMF containing 0.01 M LiBr at a flow rate of 1.0 mL/min at 50 °C. Monodispersed polystyrene standards purchased from Waters with a molecular weight range of 1790 to 2.0 × 10^5 were used to generate the calibration curve. The ellipticity of polymer aqueous solution (0.05 wt %) was obtained on a JASCO J-810 spectrometer as a function of temperature in the range of 10−50 °C. TEM measurement was performed on a JEOL JEM-1011 transmission electron microscope with an accelerating voltage of 100 KV. PEG_{45}-$PELG_{12}$ aqueous solutions (0.5 g L^{-1}) were kept at 20 and 37 °C for 20 min, respectively. Then a drop of polypeptide aqueous solution was deposited onto a 230 mesh copper grid coated with carbon and allowed to dry at 20 and 37 °C, respectively, before measurement. DLS measurements were performed on a WyattQELS instrument with a vertically polarized He−Ne laser (DAWN EOS, Wyatt Technology) and 90° collected optics. The sample was prepared in aqueous solution at a concentration of 1 wt %. Before measurements, the solution was filtered through a 0.45 μm Millipore filter. Fluorescence excitation spectra were recorded on a Perkin-Elmer LS50B luminescence spectrometer at the detection wavelength (λ_{em}) of 390 nm.

Synthesis of γ-Alkyl-L-glutamates. To a mixture of L-glutamic acid (20 g) and methanol (30 mL), 8 mL of sulfuric acid was added dropwise over 30 min at room temperature. After stirring at room temperature overnight, the viscous solution was poured slowly into the mixture of ethanol and triethylamine to yield white precipitate. The crude product was recrystallized from water and ethanol to obtain γ-methyl-L-glutamate (MLG; 10.9 g, 50% in yield). γ-Ethyl-L-glutamate (ELG), γ-propyl-L-glutamate (PLG), and γ-butyl-L-glutamate (BLG) were synthesized in a similar procedure with yields of 61, 72, and 59%, respectively.

Synthesis of γ-Alkyl-L-glutamates *N*-Carboxyanhydrides. MLG (3.22 g, 20 mmol) and triphosgene (1.98 g, 6.7 mmol) were suspended in 100 mL of dry THF bubbled with nitrogen flux in a flame-dried three-neck flask. The mixture was stirred at 50 °C for 1 h. After further bubbling with nitrogen flux for 30 min, the solution was precipitated into 400 mL of petroleum ether and stored at −20 °C overnight. After removing the supernatant, the residues were collected and dissolved in 100 mL of ethyl acetate, followed by washing with 50 mL of ice-cold water twice and 50 mL of 0.5% $NaHCO_3$ ice-cold aqueous solution. The organic phase was then dried over anhydrous $MgSO_4$ and evaporated to give γ-methyl-L-glutamate *N*-carboxyanhydride (MLG NCA; 2.17 g, 58% in yield). γ-Ethyl-L-glutamate *N*-carboxyanhydride (ELG NCA), γ-propyl-L-glutamate *N*-carboxyanhydride (PLG NCA), and γ-butyl-L-glutamate *N*-carboxyanhydride (BLG NCA) were synthesized in a similar procedure with yields of 66, 52, and 49%, respectively.

Synthesis of Poly(ethylene glycol)-*block*-poly(γ-alkyl-L-glutamate)s. The PEG-polypeptide diblock copolymers were synthesized through the ring-opening polymerization of γ-alkyl-L-glutamate *N*-carboxyanhydrides using amino-terminated mPEG (denoted as $mPEG_{45}$-NH_2) as macroinitiator. A typical procedure for the preparation of poly(ethylene glycol)-*b*-poly(γ-ethyl-L-glutamate) (PEG_{45}-$PELG_{12}$) was as follows: $mPEG_{45}$-NH_2 (1 g, 0.5 mmol) was dissolved in toluene (100 mL) and residual water in the solution was removed by azeotropic distillation. Anhydrous *N*,*N*-dimethylamide (20 mL) and γ-ethyl-L-glutamate *N*-carboxyanhydride (ELG NCA; 1.51 g, 7.5 mmol) were then added to the flask. The reaction mixture was stirred at 25 °C for 3 days under a dry nitrogen atmosphere. Then the copolymer was purified by precipitated into glacial diethyl ether, followed by filtration. The obtained product was further washed twice with diethyl ether and dried under vacuum. The yield was 65%. Poly(ethylene glycol)-*b*-poly(γ-methyl-L-glutamate) (PEG_{45}-$PMLG_{12}$), poly(ethylene glycol)-*b*-poly(γ-propyl-L-glutamate) (PEG_{45}-$PPLG_{10}$), and poly(ethylene glycol)-*b*-poly(γ-butyl-L-glutamate) (PEG_{45}-$PBLG_9$) were synthesized in a similar procedure with the yields of 71, 49, and 52%, respectively.

Phase Diagram. The sol−gel transition behavior of the copolymers in phosphate buffered saline (PBS, pH 7.4) was determined by the inverting test method with a temperature increment of 1 °C per step. Each sample at a given concentration was dissolved in PBS and stirred at 0 °C for 24 h. The copolymer solution (0.5 mL) was introduced to the test tube with an inner diameter of 11 mm. The sol−gel transition temperature was recorded if no flow was observed within 30 s after inverting the test tube. Each data point was the average of three measurements.

Dynamic Mechanical Analysis. Rheology experiments were performed on a US 302 Rheometer (Anton Paar). The copolymer solution was placed between parallel plates of 25 mm diameter and a gap of 0.5 mm. To prevent the evaporation of water, the outer edge of the sandwiched sample was sealed by a thin layer of silicon oil. The data were collected under a controlled strain γ of 1% and a frequency of 1 rad/s. The heating rate was 0.5 °C/min.

In Vivo Gel Formation. Sprague−Dawley (SD) rats (about 200 g) were used for the in vivo gel formation. Rats were anesthetized by inhalation of diethyl ether, and 0.2 mL of PEG_{45}-$PELG_{12}$ PBS solution (6.0 wt %) was subcutaneously injected into dorsal areas of rats with a 21-gauge needle. After 10 min, the rats were sacrificed and the gel status was observed.

In Vitro Gel Duration. The PEG_{45}-$PELG_{12}$ hydrogels were obtained by incubating 0.5 mL copolymer solutions in PBS (6.0 wt %) within different vials (diameter = 16 mm) at 37 °C for 10 min. Tris-HCl buffer solution (0.05 M, pH 7.4) containing 0.2 mg/mL proteinase K, 10 mM $CaCl_2$, and 0.2 wt % NaN_3 was used as the degradation media, and hydrogels incubated in Tris-HCl buffer solutions only were used as controls. The buffer solution (3.0 mL) was added on the top of the gels at 37 °C and the whole medium was replaced every day. The mass of the remaining gel was measured every day.

Cytotoxicity Measurement. The relative cytotoxicity was assessed by methyl thiazolyl tetrazolium (MTT) viability assay against HeLa cells. The cells were seeded in 96-well plates at 10,000 cells per well in 100 μL of complete Dulbecco's modified Eagle's medium (DMEM) containing 10% fetal bovine serum, supplemented with 50 U/mL penicillin, and 50 U/mL streptomycin, and incubated at 37 °C in 5% CO_2 atmosphere for 24 h, followed by removing culture medium and adding copolymer solutions (100 μL in complete DMEM medium) at different concentrations (0.01−0.5 g L^{-1}). The cells were

Scheme 1. Synthetic Routes of Poly(ethylene glycol)-*b*-poly(L-glutamate)s with Different Side Groups

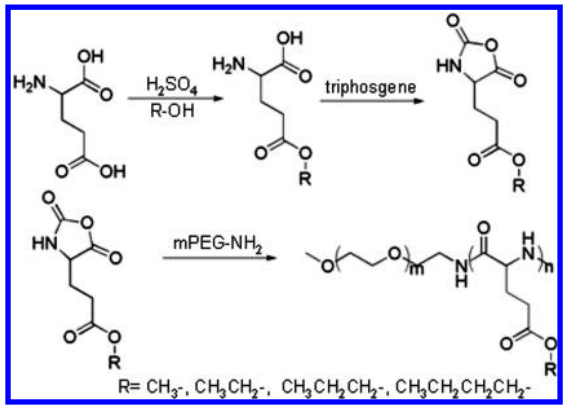

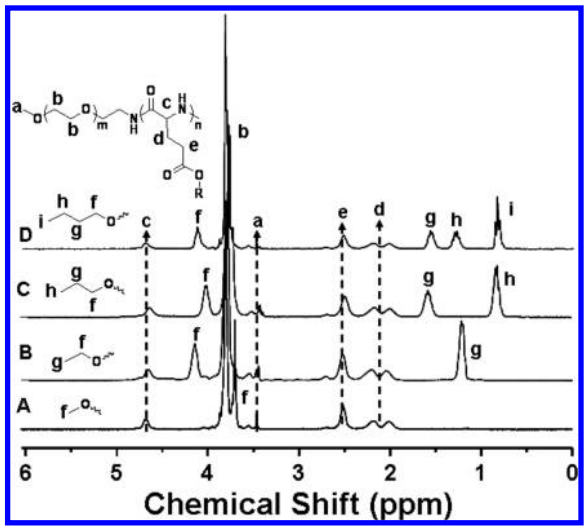

Figure 1. ^{1}H NMR spectra of (A) PEG_{45}-$PMLG_{12}$, (B) PEG_{45}-$PELG_{12}$, (C) PEG_{45}-$PPLG_{10}$, and (D) PEG_{45}-$PBLG_9$ in CF_3COOD.

subjected to MTT assay after being incubated for another 24 h. The absorbance of the solution was measured on a Bio-Rad 680 microplate reader at 492 nm. Cell viability (%) was calculated according to the following equation: cell viability (%) = $(A_{sample}/A_{control}) \times 100\%$, where A_{sample} and $A_{control}$ were the absorbances of the sample and control well, respectively. The measurements were performed in triplicate.

Animal Procedure. The experiments on animals were carried out according to the guide for the care and use of laboratory animals, provided by Jilin University, Changchun, China, and the procedure was approved by the local Animal Ethics Committee.

RESULTS AND DISCUSSION

Four kinds of L-glutamate *N*-carboxyanhydrides (LG NCA) with different alkyl protecting groups, including methyl, ethyl, *n*-propyl, and *n*-butyl, were first synthesized using triphosgene in THF, and various PEG-*b*-poly(L-glutamate)s were then fabricated by ring-opening polymerization (ROP) of the NCA monomers, separately, using $mPEG_{45}$-NH_2 as macroinitiator (Scheme 1). Typical ^{1}H NMR spectra of the block copolymers are shown in Figure 1 and all peaks have been well assigned. The degree of polymerization (DP) of poly(L-glutamate)s was calculated by comparing the integration of the methyl peak of the side groups ($-CH_3$) with that of the methylene peak of poly(ethylene glycol) ($-CH_2CH_2O-$). To compare their thermal gelling behaviors, the resulting copolymers had similar molecular weights about 3700 Da. The polydispersities (PDIs) determined by GPC were in the range of 1.1−1.3, indicating that the copolymers were all well prepared.

These block copolymers were found to assemble into micelles in water and their critical micelle concentrations (CMC) were investigated using the pyrene-probe-based fluorescence technique.[25] The excitation spectra of pyrene as the function of the concentration of the copolymers were measured. Figure S1 shows the fluorescence excitation spectra of pyrene in the PEG_{45}-$PELG_{12}$ solutions at different concentrations. A red shift of (0, 0) absorption band from 334 to 337 nm was observed when the concentration of the copolymer increased from 0.124 to 5.08×10^2 mg L^{-1}. This red shift was resulted from the transfer of pyrene molecules from water environment to the hydrophobic core, indicating the formation of amphiphilic micelles. In addition, from the plot of fluorescence intensity ratio of I_{337}/I_{334} versus $\log_{10} c$ of the polymers (Figure 2A), the CMC values were obtained. As listed

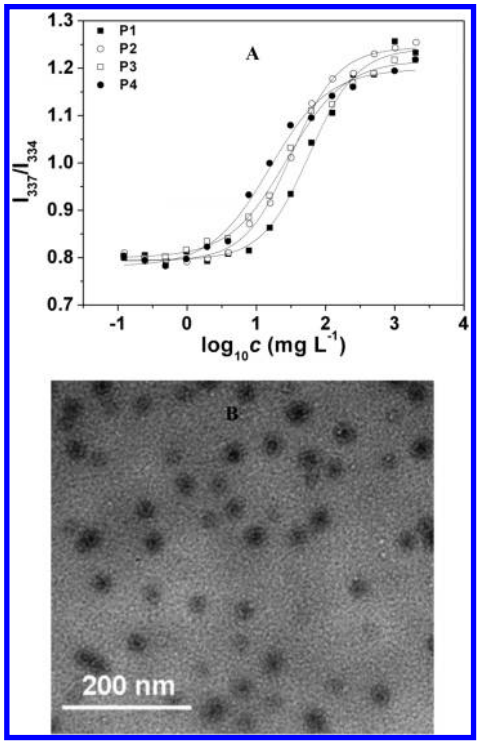

Figure 2. (A) Intensity ratio of I_{337}/I_{334} as a function of concentration of all the copolymers; (B) TEM image of PEG_{45}-$PELG_{12}$ micelles formed at 20 °C. Scale bar = 200 nm.

in Table 1, their CMC values decreased from 12.5 to 2.36 mg L^{-1} as the side group changed from methyl to *n*-butyl, which indicated that a longer side chain led to a lower CMC value due to its stronger hydrophobicity. The formation of micelles was observed by TEM at 20 °C, and the typical micrograph of PEG_{45}-$PELG_{12}$ micelles is shown in Figure 2B, which took spherical shape with the diameter of about 20 nm. When the temperature increased to 37 °C, cylindrical aggregates were observed (Figure S2), which may be related to the change in secondary structure of the polypeptide.[23]

The concentrated polypeptide solutions in PBS underwent sol−gel phase transitions as the temperature increased, and the transition temperatures were determined by the test tube inversion method.[26] The sample is regarded as a gel if no flow was observed within 30 s after the vial was inverted. The phase

dx.doi.org/10.1021/bm3004308 | *Biomacromolecules* 2012, 13, 2053−2059

Table 1. Characterizations of the Block Copolymers

code	copolymers	feeding molar ratio of NCA/mPEG$_{45}$-NH$_2$	DP[a]	M_n[a]	M_n[b]	PDI[b]	CMC (mg L^{-1})
P1	PEG$_{45}$-PMLG$_{12}$	15	12	3700	6700	1.2	12.5
P2	PEG$_{45}$-PELG$_{12}$	15	12	3800	6900	1.1	8.71
P3	PEG$_{45}$-PPLG$_{10}$	15	10	3700	6400	1.2	5.23
P4	PEG$_{45}$-PBLG$_9$	15	9	3700	5600	1.3	2.36

[a]Determined by ^{1}H NMR. [b]Determined by GPC.

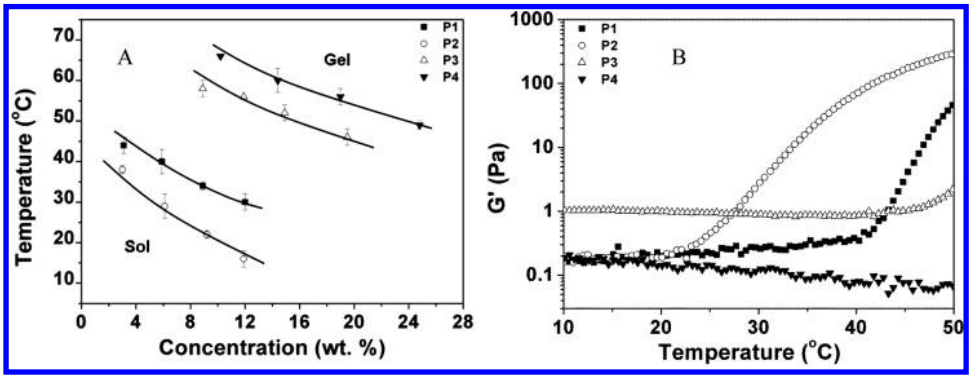

Figure 3. (A) Sol−gel phase diagrams of the block copolymer solutions (P1: PEG$_{45}$-PMLG$_{12}$; P2: PEG$_{45}$-PELG$_{12}$; P3: PEG$_{45}$-PPLG$_{10}$; P4: PEG$_{45}$-PBLG$_9$). (B) Storage moduli of 6.0 wt % PBS solutions of the PEG-polypeptides (G') as a function of temperature.

diagrams of these block copolymers with different side chains are shown in Figure 3A. All the copolymers underwent sol−gel transitions. It was noticeable that PEG$_{45}$-PPLG$_{10}$ (P3) and PEG$_{45}$-PBLG$_9$ (P4) showed much higher sol−gel transition temperatures than PEG$_{45}$-PMLG$_{12}$ (P1) and PEG$_{45}$-PELG$_{12}$ (P2). For example, at a fixed concentration of 9 wt %, P1, P2, P3, and P4 exhibited critical gelation temperatures (CGTs) at 34, 22, 58, and 62 °C, respectively.

Thermoinduced changes in storage modulus (G') of 6.0 wt % PBS solutions of the four copolymers obtained by dynamic mechanical analysis are shown in Figure 3B. Sharp increments of the G's of P1 and P2 were observed as the temperature increased. In contrast, only a slight increase in G' was observed for P3 and no obvious increase in G' was detected for P4 as the temperature increased to about 50 °C, indicating no sol−gel transition for P3 and P4 within the experimental temperature range. It has been reported that the CGT of hydrophobically end-capped poly(alanine)-(propylene glycol)-(ethylene glycol)-(propylene glycol)-poly(alanine) (PA-PLX-PA) decreased as the terminal group changed from methyl to propyl due to an increase in hydrophobicity. Notably, the increase in the length of the hydrophobic side group exhibited markedly different influence on the gelation behavior of the PEG-polypeptide block copolymers from the end-capped PA-PLX-PA systems. As shown in Figure 3A, the CGT decreased as the side group changed from methyl to ethyl group, whereas the CGT showed an abrupt increment with the further increase of the side chain length by replacing ethyl side group with either *n*-propyl or butyl group. This suggested a quite different gelation mechanism from the end-capped PA-PLX-PA systems.[23]

It is well accepted that the crossover point of the storage modulus (G') and loss modulus (G'') in the dynamic mechanical analysis reflects the sol−gel transition.[27] G' is an elastic component of the complex modulus and is a measure of the gel-like behavior of a system, whereas G'' is a viscous component of the complex modulus and is a measure of the sol-like behavior of the system. As shown in Figure S3, G' was lower than G'' in the low temperature range, indicating a viscous state. On the other hand, a significant increase in G' was observed with increasing temperature, while the increase in G'' was relatively slow, which indicated the gel formation. The transition temperature obtained from the cross point of G' and G'' coincided well with that determined by test tube method.

The solution phase behaviors of the four copolymers at a concentration of 6.0 wt % were investigated at 15, 37, and 60 °C, respectively. At 15 °C, all the copolymers dispersed well in PBS. Nevertheless, P1 and P2 formed clear solutions in PBS, whereas P3 and P4 led to cloudy solutions. When the temperature increased to 37 °C, free-standing gels were observed for P2 compared to the remaining sol states for P3 and P4. In addition, the viscosity of P1 increased. As the temperature increased to 60 °C, rigid gels were formed for P1, and P2 was still retained in the gel state. However, P3 and P4 precipitated from the solutions instead of forming hydrogels. Typical photographs of the PEG$_{45}$-PELG$_{12}$ solutions in PBS (6.0 wt %) at 15, 37, and 60 °C are shown in Figure 4, respectively.

Figure 4. Photographs of the 6.0 wt % PEG$_{45}$-PELG$_{12}$ solutions in PBS at 15, 37, and 60 °C, respectively.

To investigate the mechanism of the sol−gel transitions, ^{13}C NMR, DLS, and circular dichroism (CD) were applied to test the conformation evolution of the PEG domains and polypeptide as a function of temperature. It has been proposed that micellar aggregation at CGT caused by both an increase in interactions between the hydrophobic blocks and partial dehydration of the PEG shell might be responsible for the sol−gel transitions of some typical amphiphilic block copolymer systems.[28,29] In the present work, we investigated

the conformation change of the PEG block with changing temperature. As the temperature increased from 20 to 60 °C, the peak ascribed to PEG at 69.5−71.5 ppm became broader and shifted downfield (Figure 5), suggesting that the gradual dehydration of PEG blocks occurred during the thermoinduced sol−gel transition.

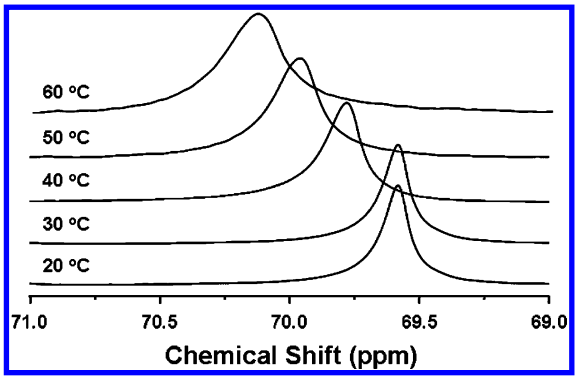

Figure 5. ^{13}C NMR spectra of 6.0 wt % PEG_{45}-$PELG_{12}$ solution in D_2O as a function of temperature.

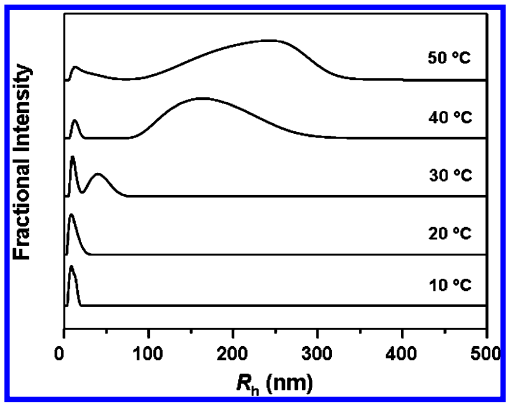

Figure 6. Distribution of hydrodynamic radius (R_h) of micelles of PEG_{45}-$PELG_{12}$ (P2) as a function of temperature in water (1.0 wt %).

To investigate the change in aggregation behavior of the block copolymers, we studied the change in micelle radius by DLS as a function of temperature (Figure 6). At the low temperature range (10−20 °C), the average radius of P2 micelles was about 15 nm, whereas the micelles began to form larger aggregates when the temperature increased to 30 °C with a broader size distribution. At above 40 °C, significant increases in both the radius and the size distribution of the aggregates were observed. It may be caused by the dehydration of the PEG shell and the interactions between micelles. These results indicated that the aggregation between micelles emerged during the sol−gel transition.[30]

The CD spectra of the P2 aqueous solution showed a positive Cotton band at 195 nm and a negative Cotton band at 210−220 nm, which are two characteristic Cotton bands corresponding to β-sheet conformation.[31] Moreover, the negative band at 216 nm was found to increase as the temperature increased from 10 to 50 °C (Figure 7). The results suggested that the increment of β-sheet conformation may be associated with the gelation.

Based on the discussions in the previous section, the change in β-sheet fraction might be one of the major causes for the phase transitions. To investigate the secondary structure of the

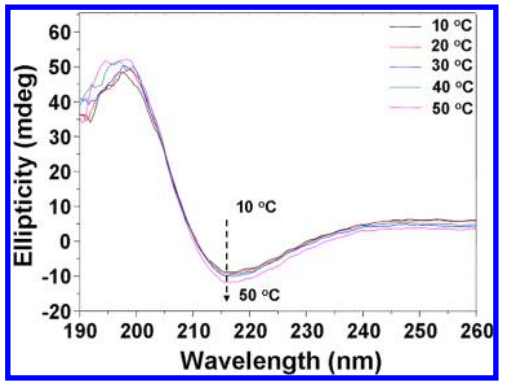

Figure 7. Circular dichroism spectra of 0.05 wt % PEG_{45}-$PELG_{12}$ aqueous solution as a function of temperature.

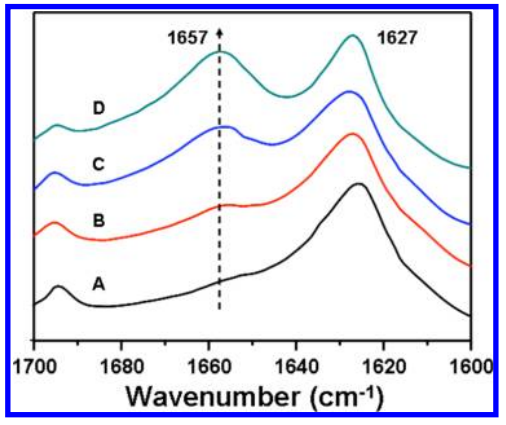

Figure 8. FTIR spectra of (A) PEG_{45}-$PMLG_{12}$, (B) PEG_{45}-$PELG_{12}$, (C) PEG_{45}-$PPLG_{10}$, and (D) PEG_{45}-$PBLG_9$ in the solid state.

resulting copolymers, FTIR spectra were performed in the solid state. As shown in Figure 8, a sharp absorption band at 1627 cm^{-1} was observed, which indicated that all copolymers adopted predominate β-sheet conformation.[32] On the other hand, the absorption band at 1657 cm^{-1}, suggesting an α-helical conformation, increased when the side group changed from methyl to *n*-butyl.[33] It demonstrated that the increase in the side group length promoted the secondary conformation transition from β-sheet to α-helix.[34] Meanwhile, ATR-FTIR was used to analyze the amide I band at 1600−1700 cm^{-1} to study the secondary structure in the solution state.[35] The results are listed in Table 2, and deconvolution of the amide I

Table 2. Percentage Content of Secondary Structures of the Polypeptides

code		helix (%)	β-sheet (%)	random coil (%)	others (%)
P1	PEG_{45}-$PMLG_{12}$	5	88	3	4
P2	PEG_{45}-$PELG_{12}$	10	85	2	3
P3	PEG_{45}-$PPLG_{10}$	26	70	1	3
P4	PEG_{45}-$PBLG_9$	30	63	2	5

band in the FTIR spectra of P2 (6.0 wt % in D_2O) is shown in Figure S4. As the side group changed from methyl to *n*-butyl, the fraction of β-sheet conformation decreased from 88 to 63% while the α-helix content increased from 5 to 30%. The conformation of β-sheet arises from the intermolecular hydrogen binding, in contrast to the intramolecular hydrogen bonding in α-helix. The increase in intermolecular interactions

dx.doi.org/10.1021/bm3004308 | *Biomacromolecules* 2012, 13, 2053−2059

is believed to be related to gel formation. Hence, the higher β-sheet of P1 and P2 (about 20% more than P3 and P4) showed markedly lower sol−gel transition temperatures than P3 and P4. In contrast, the contents of β-sheet of P1 and P2 were comparable (only 3% difference), so the lower CGT of P2 compared to P1 may be caused by higher hydrophobic interactions between the ethyl side groups.

For practical biomedical applications, polymer solutions should be easily mixed with drugs, bioactive molecules or cells at a lower temperature, and form hydrogels in situ immediately after injection into body without premature diffusion of the cargos. The in vivo gel formation was confirmed by subcutaneous injection of the PEG_{45}-$PELG_{12}$ solutions into SD rats with a 21-gauge needle. At 15 °C, the polymer solutions exhibited low viscosity and could be easily injected through the syringe needle. By contrast, free-standing gels were observed in situ 10 min after injection (Figure S5). Thus, the present polypeptide-based injectable hydrogels may be suitable candidates for localized drug and cell delivery.

The mass loss of in situ formed thermosensitive hydrogels is mainly driven by the surface erosion of the hydrogels and/or the degradation of the polymer chains.[22] The in vitro duration of P2 hydrogels (6.0 wt %) was evaluated in the presence of proteinase K. Over 90% mass loss was observed for the gels incubated with proteinase K compared to only 15% mass loss for the control group after 7 days of degradation (Figure 9).

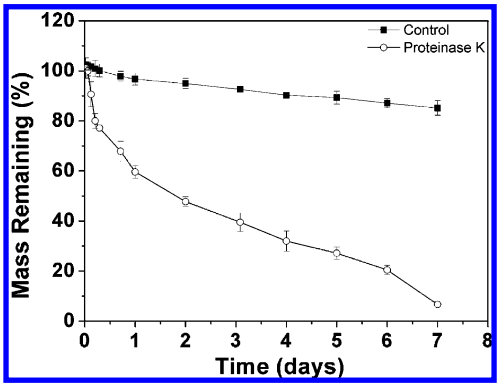

Figure 9. In vitro mass loss profiles for the in situ formed hydrogels of PEG_{45}-$PELG_{12}$ (6.0 wt %) incubated in 0.05 M Tris-HCl buffer (pH 7.4) containing 0.2 mg mL^{-1} proteinase K and in Tris-HCl buffer without proteinase K as control, respectively.

For the gels in Tris-HCl buffer without proteinase K, the mass loss was mainly attributed to surface erosion of the gels; however, in the presence of proteinase K, not only surface erosion of the gels but also the fast degradation of polypeptide chains were responsible for the faster mass loss of the hydrogels.

In addition, in vitro cytotoxicity of the block copolymers was evaluated by MTT assay.[36] The cells were treated with the copolymers at different concentrations for 24 h, and PEI 25K was used as positive control. The relative cell viabilities are shown in Figure S6. It was observed that the HeLa cells treated with the copolymers remained almost 100% viable at all concentrations up to 0.5 g L^{-1}, indicating good biocompatibility of the block copolymers.

CONCLUSIONS

Four block copolymers based on PEG and poly(L-glutamate)s bearing different hydrophobic side groups were synthesized through ROP of L-glutamate NCA monomers, and an interesting effect of the side group on the solution phase behavior was observed. The concentrated solutions of the resulting copolymers underwent a sol−gel transition as a function of temperature. Noticeably, the polypeptides containing methyl and ethyl groups showed much lower CGTs than those bearing *n*-propyl and butyl side groups, which was due to the higher β-sheet contents for the former systems with shorter side chains. On the other hand, for the polypeptides with comparable β-sheet contents (P1 and P2), the increase in hydrophobicity could lead to a slightly decrease in the sol−gel transition temperature. The present work revealed that subtle variation in the length of hydrophobic side group displayed significant effect on the secondary conformation and gelation behavior of the thermosensitive polypeptide block copolymers, which might give valuable insights into the gelation mechanisms as well as the role of secondary structure of polypeptides in promoting gelation. Moreover, the biocompatible and biodegradable in situ gelling hydrogels may be promising candidates for applications in localized drug and cell delivery.

ASSOCIATED CONTENT

Supporting Information

The excitation spectra of pyrene in PEG_{45}-$PELG_{12}$ aqueous solutions (Figure S1), TEM image of PEG_{45}-$PELG_{12}$ micelles formed at 37 °C (Figure S2), dynamic mechanical analysis of PEG_{45}-$PELG_{12}$ PBS solution (Figure S3), deconvolution of the FTIR spectra of PEG_{45}-$PELG_{12}$ aqueous solution (Figure S4), the photograph of the in situ formed hydrogels (Figure S5), and in vitro cytotoxicities of the block copolymers (Figure S6). This material is available free of charge via the Internet at http://pubs.acs.org.

AUTHOR INFORMATION

Corresponding Author

*E-mail: xschen@ciac.jl.cn.

Notes

The authors declare no competing financial interest.

ACKNOWLEDGMENTS

The authors are grateful for the financial support from the National Natural Science Foundation of China (Projects 51003103, 21174142, 50973108, and 51021003), the Ministry of Science and Technology of China (International Cooperation and Communication Program 2010DFB50890), and the Scientific Development Program of Jilin Province (201101082, 20110332).

REFERENCES

(1) He, C.; Zhuang, X.; Tang, Z.; Tian, H.; Chen, X. *Adv. Healthcare Mater.* **2012**, *1*, 48−78.
(2) Yu, L.; Ding, J. D. *Chem. Soc. Rev.* **2008**, *37*, 1473−1481.
(3) Park, M. H.; Joo, M. K.; Choi, B. G.; Jeong, B. *Acc. Chem. Res.* **2012**, *3*, 424−433.
(4) He, C. L.; Kim, S. W.; Lee, D. S. *J. Controlled Release* **2008**, *127*, 189−207.
(5) Huynh, C. T.; Nguyen, M. K.; Lee, D. S. *Macromolecules* **2011**, *44*, 6629−6636.
(6) Jeong, B.; Bae, Y. H.; Lee, D. S.; Kim, S. W. *Nature* **1997**, *388*, 860−862.
(7) Lee, J.; Bae, Y. H.; Sohn, Y. S.; Jeong, B. *Biomacromolecules* **2006**, *7*, 1729−1734.

(8) Yu, L.; Zhang, H.; Ding, J. D. *Angew. Chem., Int. Ed.* **2006**, *45*, 2232−2235.
(9) Yu, L.; Zhang, Z.; Ding, J. D. *Biomacromolecules* **2011**, *12*, 1290−1297.
(10) Gong, C. Y.; Shi, S. A.; Wu, L.; Gou, M. L.; Yin, Q. Q.; Guo, Q. F.; Dong, P. W.; Zhang, F.; Luo, F.; Zhao, X.; Wei, Y. Q.; Qian, Z. Y. *Acta Biomater.* **2009**, *5*, 3358−3370.
(11) Shim, W. S.; Kim, S. W.; Lee, D. S. *Biomacromolecules* **2006**, *7*, 1935−1941.
(12) Loh, X. J.; Goh, S. H.; Li, J. *Biomacromolecules* **2007**, *8*, 585−593.
(13) Nguyen, M. K.; Park, D. K.; Lee, D. S. *Biomacromolecules* **2009**, *10*, 728−731.
(14) Malmsten, M. *Soft Matter* **2006**, *2*, 760−769.
(15) Yu, L.; Chang, G. T.; Zhang, H.; Ding, J. D. *Int. J. Pharm.* **2008**, *348*, 95−106.
(16) Cao, Y. L.; Rodriguez, A.; Vacanti, M.; Ibarra, C.; Arevalo, C.; Vacanti, C. A. *J. Biomater. Sci., Polym. Ed.* **1998**, *9*, 475−487.
(17) Nowak, A. P.; Breedveld, V.; Pakstis, L.; Ozbas, B.; Pine, D. J.; Pochan, D.; Deming, T. J. *Nature* **2002**, *417*, 424−428.
(18) Deacon, S. P. E.; Apostolovic, B.; Carbajo, R. J.; Schott, A. K.; Beck, K.; Vicent, M. J.; Pineda-Lucena, A.; Klok, H. A.; Duncan, R. *Biomacromolecules* **2011**, *12*, 19−27.
(19) Rathore, O.; Sogah, D. Y. *J. Am. Chem. Soc.* **2001**, *123*, 5231−5239.
(20) Vandermeulen, G. W. M.; Tziatzios, C.; Duncan, R.; Klok, H. -A. *Macromolecules* **2005**, *38*, 761−769.
(21) Kim, E. H.; Joo, M. K.; Bahk, K. H.; Park, M. H.; Chi, B.; Lee, Y. M.; Jeong, B. *Biomacromolecules* **2009**, *10*, 2476−2481.
(22) Moon, H. J.; Choi, B. G.; Park, M. H.; Joo, M. K.; Jeong, B. *Biomacromolecules* **2011**, *12*, 1234−1242.
(23) Kim, J. Y.; Park, M. H.; Joo, M. K.; Lee, S. Y.; Jeong, B. *Macromolecules* **2009**, *42*, 3147−3151.
(24) Ding, J. X.; Shi, F. H.; Xiao, C. S.; Lin, L.; Chen, L.; He, C. L.; Zhuang, X. L.; Chen, X. S. *Polym. Chem.* **2011**, *2*, 2857−2864.
(25) Cheng, Y.; He, C.; Xiao, C.; Ding, J.; Zhuang, X.; Chen, X. *Polym. Chem.* **2011**, *2*, 2627−2634.
(26) Tanodekaew, S.; Godward, J.; Heatley, F.; Booth, C. *Macromol. Chem. Phys.* **1997**, *198*, 3385−3395.
(27) Sarvestani, A. S.; He, X. Z.; Jabbari, E. *Biomacromolecules* **2007**, *8*, 406−415.
(28) Yu, L.; Chang, G. T.; Zhang, H.; Ding, J. D. *J. Polym. Sci., Part A: Polym. Chem.* **2007**, *45*, 1122−1133.
(29) Wang, Y. C.; Xia, H.; Yang, X. Z.; Wang, J. *J. Polym. Sci., Part A: Polym. Chem.* **2009**, *47*, 6168−6179.
(30) Yu, L.; Zhang, Z.; Zhang, H.; Ding, J. D. *Biomacromolecules* **2009**, *10*, 1547−1553.
(31) Nuhn, H.; Klok, H. A. *Biomacromolecules* **2008**, *9*, 2755−2763.
(32) Haris, P. I.; Chapman, D. *Biopolymers* **1995**, *37*, 251−263.
(33) Blout, E. R.; Asadourian, A. *J. Am. Chem. Soc.* **1956**, *78*, 955−961.
(34) Lotan, N.; Yaron, A.; Berger, A. *Biopolymers* **1966**, *4*, 365−368.
(35) Baginska, K.; Makowska, J.; Wiczk, W.; Kasprzykowski, F.; Chmurzynski, L. *J. Pept. Sci.* **2008**, *14*, 283−289.
(36) Ding, J. X.; Xiao, C. S.; He, C. L.; Li, M. Q.; Li, D.; Zhuang, X. L.; Chen, X. S. *Nanotechnology* **2011**, *22*, 494012.